Cavitation effects versus stretch effects resulted in different size and polydispersity of ionotropic gelation chitosan–sodium tripolyphosphate nanoparticle

Min Lang Tsai, Shi Wei Bai, Rong Huei Chen *

Department of Food Science, National Taiwan Ocean University, 2, Pei-Ning Road, Keelung 20224, Taiwan, ROC

Abstract

The objectives of the study are to compare different modes and input-energy levels of ultrasonic radiation and mechanical shearing on the changes in mean diameter of resulted ionotropic gelation chitosan–sodium tripolyphosphate (TPP) nanoparticles, and to elucidate the different effects on the size and polydispersity difference caused by cavitation effects versus stretch effects owing to using different modes of mechanical energy. The results obtained were as follows: the particle size and reduction rate of ionotropic gelation chitosan–TPP can be manipulated by varying different mechanical energy of ultrasonic radiation or mechanical shearing. Effects of solution temperature on resulted nanoparticle size by ultrasonic treatment or by mechanical shearing were different. The higher the solution temperature, the lower the solution viscosity that facilitates the sporadic cavitation effect exerted on the chitosan molecules producing smaller molecular weight fragments than that produced by stretching effects. Mean diameter of nanoparticle decreased with increasing solution temperature in ultrasonic radiation samples.
© 2007 Elsevier Ltd. All rights reserved.

Keywords: Chitosan; Tripolyphosphate; Nanoparticle; Particle size; Cavitation; Stretch

1. Introduction

Chitosan is a high molecular weight polysaccharide linked by β-1,4 glycoside. It is composed by *N*-acetyl-glucosamine and glucosamine. It is considered to be the most wide distribution biopolymer, having huge resources, with cationic polyelectrolyte, non-toxic, biocompatible, and biodegradable.

Chitosan nanoparticle has attracted great attention in pharmaceutical applications including colon targeted drug delivery, mucosal delivery, cancer therapy, vaccine delivery, gene delivery, etc. because the primary amine groups render positive charge and mucoadhesive properties that make chitosan very useful in drug delivery applications (Agnihotri, Mallikarjuna, & Aminabhavi, 2004; Sarmento,

Ferreira, Veiga, & Ribeiro, 2006; Vila et al., 2004; Yuan, Li, & Yuan, 2006). Chitosan nanoparticle is a very efficient and non-toxic absorption enhancer for both orally and nasally administered peptide drug (van der Lubben, Verhoef, Borchard, & Junginger, 2001). Moreover, preliminary blood compatibility tests of chitosan nanoparticle showed that the long aliphatic and aromatic acyl groups did not significantly influence the hemolytic activity and blood clotting behavior (Lee, Powers, & Baney, 2004). Furthermore, the potential use of polymeric nanoparticles as drug carriers has led to the development of many different colloidal delivery vehicles. The main advantages of these kind of systems lie in their capacity to cross biological barriers, to protect macromolecules, such as peptides, proteins, oligonucleotides, and genes from degradation in biological media, and to deliver drugs or macromolecules to a target site with following controlled release (López-León, Carvalho, Seijo, Ortega-Vinuesa, & Bastos-González, 2005). Desai, Labhasetwar, Walter, Levy, and Amidom (1997)

* Corresponding author. Tel.: +886 2 2462 2192x5104; fax: +886 2 2463 1977.
E-mail address: rhchen@mail.ntou.edu.tw (R.H. Chen).

reported that particle uptake by caco-2 cell depends significantly upon the particle's diameter. The 100 nm diameter particles had 2.5-fold greater uptakes on the weight basis than the 1 μm and 6-fold greater than the 10 μm diameter particles. Similarly in terms of number the uptake of 100 nm diameter particles was 2.7×10^3-fold greater than the 1 μm and 6.7×10^6-fold greater than the 10 μm diameter particles.

The ionotropic gelation method is commonly used to prepare chitosan nanoparticle. In acidic solution, the –NH_2 of chitosan molecule is protonized to be –NH_3^+, it interacts with an anion such as tripolyphosphate (TPP) by ionic interaction to form microgel particle (Lee, Mi, Shen, & Shyu, 2001). This method is very simple and mild. In addition, reversible physical crosslinking by electrostatic interaction, instead of chemical crosslinking, is applied to prevent possible toxicity of reagents and other undesirable effects (Shu & Zhu, 2000).

However, studies on the effect of preparation conditions on particle size or stability of nanoparticle are rare. Grenha, Seijo, and Remuñán-López (2005) reported that chitosan nanoparticles were prepared with different concentrations of chitosan solutions. Their results showed the high concentration chitosan solution formed larger size particle. Gan, Wang, Cochrane, and McCrron (2005) reported that variations in chitosan molecular weight, chitosan concentration, chitosan to TPP weight ratio, and solution pH value were examined systematically for their effects on nanoparticle size, intensity of surface charge, and tendency of particle aggregation so as to enable speedy fabrication of chitosan nanoparticles with predetermined properties. They reported that at the same concentration of chitosan solution (between 0.5 and 3.0 mg/ml), the mean particle size of chitosan–TPP nanoparticle increased with increasing M_w of chitosan used. Calvo, Remunan-Lopez, Vila-Jato, and Alonso (1997) reported that size and zeta potential of chitosan–TPP nanoparticles can be conveniently modulated by varying the ratio chitosan/ethylene oxide and propylene oxide. Lan, Yang, and Li (2004) reported that the agglomerates of SiC nanoparticles by ultrasonics have greatly improved when compared with the severe agglomerates in composites fabricated by traditionally mechanical stirring. Cao, Zhang, and Huang (2005) reported the particle size and morphology of hydroxyapatite nanoparticle were modulated with different ultrasonic powers.

Tang, Huang, and Lim (2003) reported method to manipulate the nanoparticle size after chitosan nanoparticle was prepared with ionotropic gelation. The prepared chitosan nanoparticles were ultrasonicated at increasing reaction time or radiation amplitude to decrease the mean diameter and polydispersity of the nanoparticles.

The objectives of this study are to explore different effects of cavitation versus stretching exerted by ultrasonic radiation and by mechanical stretch, respectively, different energy input, solution temperatures, reaction times, and chitosan concentrations on size and polydispersity of

resulted chitosan–TPP nanoparticle and their stability. This report only address to the effect of size and polydispersity. The second part will addresses to the effects on the storage stability of these nanoparticles in different buffer solutions.

2. Materials and methods

2.1. Chitosan preparation

Squid pens were donated as a gift from Shin Dar Bio-Tech. Co. Ltd (Taiwan). The modified procedure of Kurita, Tomita, Ishii, Nishimura, and Shimoda (1993) was used to prepare the β-chitin. In brief squid pens were ground to 40–60 mesh size. Each 100 g of powder was immersed in 500 ml of 1 M hydrochloric acid solution overnight. The powder was washed to neutrality and drained. The powder was soaked in 500 ml of 2 M sodium hydroxide at ambient temperature overnight, then it was soaked in 500 ml of 2 M sodium hydroxide solution at 100 °C for 4 h, washed and dried to produce about 35 g β-chitin.

β-Chitin was added to 50% (w/w) sodium hydroxide solution at a ratio of 1 (g solid):20 (ml solution). The deacetylation reaction took place at 100 °C for 1 h. Then the sample was washed to neutrality and freeze-dried (Kurita et al., 1993; Tsaih & Chen, 2003).

2.2. Degree of deacetylation measurement

Infrared spectrometry was used to determine the degree of deacetylation (DD) of the chitosans (Baxter, Dillon, Taylor, & Roberts, 1992). Chitosan powder was sieved through a 200 mesh then mixed with KBr (1:100) and pressed into a pellet. The absorbances of amide 1 (1655 cm^{-1}) and of the hydroxyl band (3450 cm^{-1}) were measured using a Bio-Rad FTS-155 infrared spectrophotometer. The band of the hydroxyl group at 3450 cm^{-1} was used as an internal standard to correct for disc thickness and for differences in chitosan concentration in making the KBr disc. The percentage of the amine group's acetylation in a sample is given by $(A_{1655}/A_{3450}) \times 115$. Here, A_{1655}, A_{3450} are the absorbances at 1650 cm^{-1} and 3450 cm^{-1}, respectively. Chitosan with a DD of 71% was used in this study.

2.3. Molecular weight determination

Size exclusion high performance liquid chromatography (SE-HPLC) method of Tsaih and Chen (1999) was followed. A column (7.8 mm × 30 cm) packed with TSK gel G4000$_{XL}$ and G5000 PW$_{XL}$ (Tosoh Co. Ltd, Japan) was used. The mobile phase consisted of 0.2 M acetic acid/0.1 M sodium acetate, and 0.008 M sodium azide. Sample concentration of 0.1% (w/v) was loaded and eluted with a flow rate of 0.6 ml/min by an LDC Analytical ConstaMetric 3500 pump. The elute peak was detected by an RI detector (Gilson model M132, USA). The data were analyzed by

a Chem-Lab software (Scientific Information Service Corporation, Taiwan). Chitosans with known molecular weight (determined by light scattering) were used as markers. The calibration curve of elution volume and molecular weight was established. The weight average molecular weights of the samples were calculated from the calibration curve with the Chem-Lab software. Chitosan with a molecular weight of 450 kDa was used in this study.

2.4. Chitosan nanoparticle preparation

Chitosan–TPP nanoparticles were prepared with modified method of López-León et al. (2005) and Tang et al. (2003). Different concentration chitosan solutions (1, 2, 4, and 10 mg/ml) with 1% (w/w) acetic acid were prepared, then, TPP solution (0.84 mg/ml) was added into chitosan solution at a volume ratio of 5:2 (v/v) (chitosan:TPP), cavitation effect is exerted by ultrasonic radiation (VCX 750, Sonic & Materials. Inc., USA), whereas the stretching effect is exerted by a mixer (G-100R, Shinguang, Taiwan). The configurations of reactor in the ultrasonicator or in the mixer used in the experiments are shown in Fig. 1. After treatment, five times volume phosphate buffer (pH 7.5) was added into chitosan–TPP solution. Larger particle was removed by $12,000 \times g$ centrifugal treatment. The supernatant contains the chitosan–TPP nanoparticle which was harvested and the mean diameter was determined by light scattering. The ultrasonic radiation was exerted at 10, 29, and 48 W input powers; for 1, 2, and 4 min; at 4, 25, and 45 °C. The stretching was exerted by a mixer at

60, 300, and 1000 rpm; for 1, 2, and 4 min; at 4, 25, and 45 °C.

2.5. Mean diameter and polydispersity determination of nanoparticles

Light scattering method was used to measure the mean diameter and polydispersity of chitosan–TPP nanoparticle. The scattered light intensity of the solution at 90° was measured by light scattering photometer (Malvern 4700, Malvern instrument, UK) with 632.8 nm at 30 ± 0.1 °C. Every sample measurement was repeated three times. The scattered light intensity was converted to the diffusion coefficient (D, m^2/s). The size of the nanoparticle was calculated from the diffusion coefficient of the particles using Stoke–Einstein equation by PCS software version 1.61:

$$R = KT/6\pi\eta D$$

where R is radius of particle (m), K is the Boltzmann constant (J/K), T is the absolute temperature (K), and η is the viscosity of the medium (Banerjee, Mitra, Singh, Sharma, & Maitra, 2002; Tsaih & Chen, 1999).

The polydispersity (p) is calculated from the diffusion coefficients by PCS software version 1.61 using the following equation:

$$p = \frac{\sqrt{\overline{D^2} - \overline{D}^2}}{\overline{D}}$$

where $\overline{D}$ is average of the diffusion coefficient (D) and $\overline{D^2}$ is average of square of the diffusion coefficient.

3. Results and discussion

3.1. Effect of input energy

Fig. 2(a) shows increased ultrasonic energy inputs, decreased mean diameter of resulted nanoparticle. The results indicated different cavitation effects exerted by different ultrasonication input energy of 10, 29, and 48 W onto 2 mg/ml chitosan solution at 25 °C, 4 min. Fig. 2(b) shows increased shearing speeds, decreased mean diameter of nanoparticle. The results showed different stretching effects exerted by a mixer shearing at 60, 300, and 1000 rpm onto 2 mg/ml chitosan solution at 25 °C, 4 min. Results in Fig. 2(c) shows that increased ultrasonic energy input decreased the polydispersity of resulted nanoparticle from 0.440 to 0.393 and to 0.388. Results in Fig. 2(d) shows that on increasing shearing speed from 60 to 300 rpm, the polydispersity decreased from 0.516 to 0.508, however, on increasing shearing speed further to 1000 rpm, the polydispersity increased only to 0.528.

Results in Fig. 2(a) or (b) shows that increased the cavitation effect or stretching effect decreased the size of resulted nanoparticle. This phenomenon is similar to the results of Cao et al. (2005) and Tang et al. (2003). Tang et al. (2003) reported that the prepared ionotropic gela-
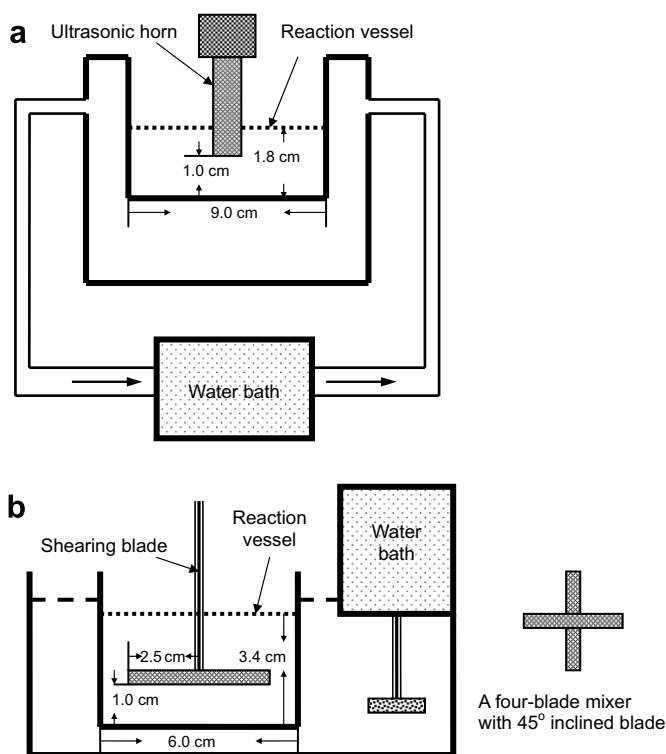

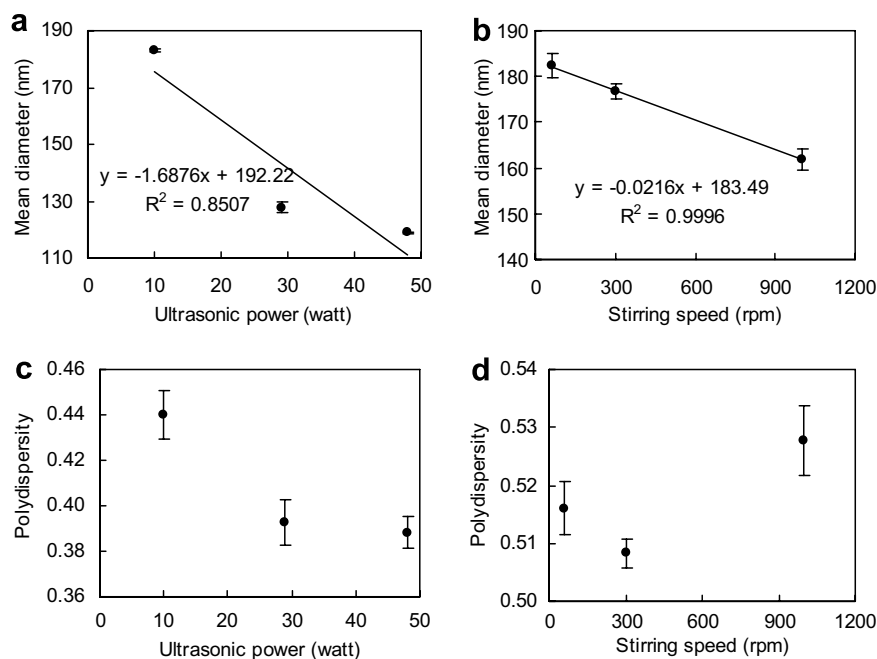Fig. 1. The configuration of reactors in (a) ultrasonicator and (b) mixer.

Fig. 2. Effects of input energy in terms of W of ultrasonic radiation (a), (c) and rpm of mechanical shearing speed (b), (d) in 2 mg/ml chitosan solution, at 25 °C, 4 min on the mean diameter (a), (b) and polydispersity (c), (d) of ionotropic gelation chitosan–sodium tripolyphosphate nanoparticles.

tion chitosan nanoparticles were ultrasonicated, the mean diameter and polydispersity of gelation chitosan nanoparticles decreased from 0.53 to 0.30 due to the bombardment of ultrasonic radiation and resulted in the breaking of nanoparticle into debris, the degree of fragmentation increased with raising of the radiation time or amplitude of ultrasonic radiation. Cao et al. (2005) report a novel ultrasonic precipitation method to prepare the hydroxyapatite nanoparticles. The size of the nanoparticle decreased linearly with increasing ultrasonic power. It indicated that the irradiation of ultrasound onto the reaction solution during the precipitation process facilitates the finer particles' formation. Results in Fig. 2(a) and (b) shows the slopes of decrease in mean particle size were different, the slope in Fig. 2(a) is steeper than that of Fig. 2(b). This may be due to different degradation mechanisms of chitosan molecules and different size of degraded chitosan molecules participating in the ionotropic gelation with TPP molecules (Fig. 3). The degradation of chitosan molecules by ultrasonic radiation is mainly caused by cavitation effect. Cavitation yields vibration wave energy, shear stress at cavitation interphase and local high pressure and temperature (Grönroons et al., 2001). Cavitation actions take place all over the solution concurrently to degrade chitosan molecular (Tsaih, Tseng, & Chen, 2004) or to break up the nanoparticle cluster to fine particle (Lan et al., 2004). The bombardment of cavitation resulted in much more chitosan debris and smaller degraded molecules than that of stretching effect exerted by mechanical shearing. The smaller fragment chitosan resulted in smaller ionotropic gelation chitosan–TPP nanoparticle (Gan et al., 2005). The number and energy of cavitation produced during ultrasonic radiation is pro-

portional to the input energy. Whereas, the degradation of chitosan molecules by shearing is mainly caused by entanglement and stretch between the entangled molecules, the torn, and stretched fragment might interact with TPP before the torn and stretched fragment has chance to wind into random coil. The mechanism of the polymer shearing degradation was proposed as the polymer sheared along the direction of shearing flow, the strong elongated flow encountered by the polymer may bring sufficient energy to disrupt the molecules. The shear stress to which the polymer is exposed exceeds a critical value specific to the polymer (Floury, Desrumaus, Axelos, & Legrand, 2002). Besides Casale and Porter (1978) report the entangled molecules facilitated the degradation reaction during shearing treatment. Therefore, the length of the polymer has to be long enough to be entangled and stretched by the shear force. The size of the torn fragment should be much bigger than the bombardment fragment, the torn chitosan may tear into half of its original size or tear into one bigger than half of its original size, another smaller than half of its original size. Whereas, the bombarded chitosan may break into several pieces depending on the number and energy level of cavitations being generated. Therefore, the mean particle size prepared by cavitation effect is smaller than that prepared by tearing effect. This can explain why decrease in mean diameter was faster in Fig. 2(a) than that in Fig. 2(b). Results of Gan et al. (2005) agree with the hypothesis of different degradation mechanism by cavitation or by stretch which will result in different size of nanoparticle as shown in Fig. 2(a) and (b). The results in Fig. 2(c) shows that increased ultrasonic energy input decreased the polydispersity of resulted nanoparticle from 0.440 to
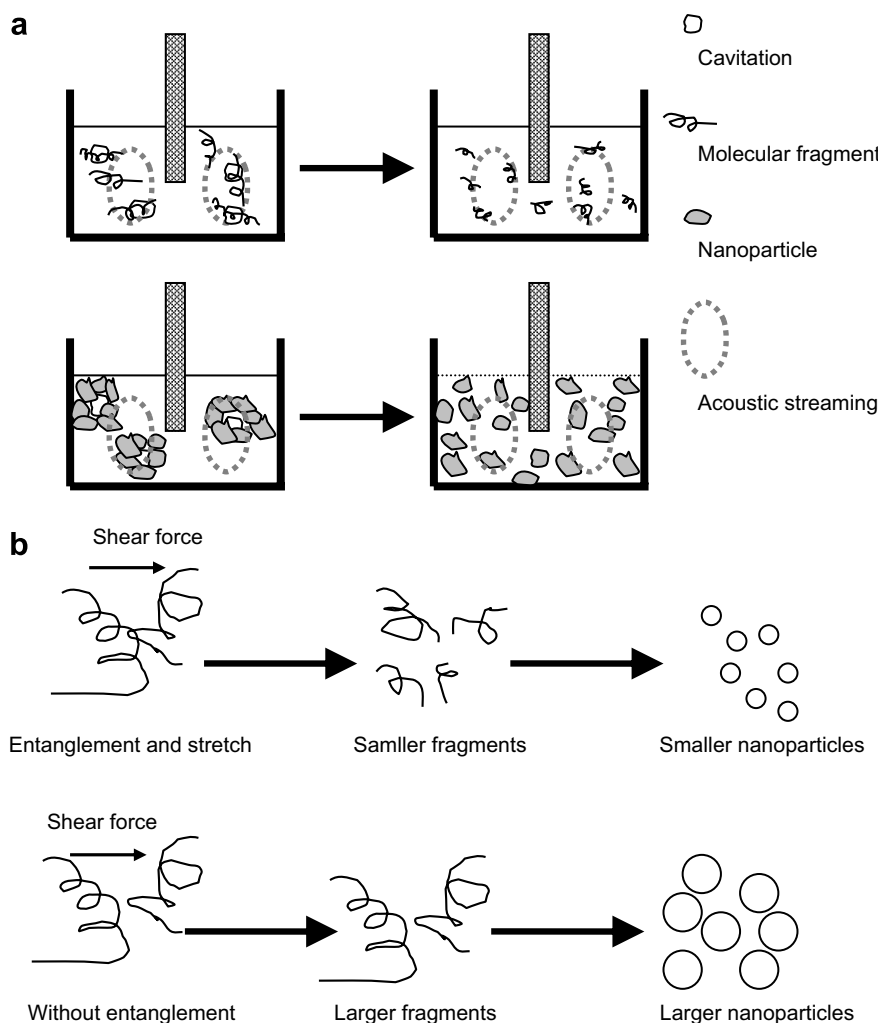
Fig. 3. Schematic diagrams illustrate the effect of ultrasonic cavitation (a) and the effect of shearing stretch (b) on nanoparticle formation.

0.393 and to 0.388. However, results in Fig. 2(d) shows that on increasing shearing speed, from 60 to 300 rpm, the polydispersity decreased from 0.516 to 0.508, however, on increasing shearing speed further to 1000 rpm, the polydispersity increased to 0.528. Effect of input energy resulted in different polydispersity pattern. This may be due to different degradation mechanisms of chitosan molecules and different size of degraded chitosan molecules participating in the ionotropic gelation with TPP molecules mentioned. The number and energy of cavitation produced during ultrasonic radiation is proportional to the input energy. Therefore, the mean diameter and polydispersity of resulted nanoparticles decreased hand in hand with increased ultrasonic power input. However, the degradation of chitosan molecules during shearing was caused mainly by stretch between the entangled molecules. Increasing shearing speed might result in different sizes of torn fragment. Although the average size of the torn fragment of chitosan decreased proportionally with increased stirring speed, however, the polydispersity of resulted nanoparticle increased due to presence of small and large fragments simultaneously, thus resulting in larg-

est polydispersity for these subjected to 1000 rpm shearing.

In our mechanical stirring system (Fig. 1(b)), the input power of mixer can be calculated as follows (Azbel & Cheremisinoff, 1983):

$$W = 0.736 \times SQ(D/d)^{0.26}, \quad S = r^2 d^3 \mu,$$
$$Q = 0.0211 \times Re^{0.88}, \quad Re = rd^2\rho/\mu$$

Here, W is the input power of mixer, S is the power coefficient, Q is the dimensionless number, Re is the modified Reynolds number, D is the beaker diameter, d is the mixer diameter, r is the rotation speed, μ is the viscosity of fluid, ρ is the density of the medium. The input energies calculated from the above equations were 1.71×10^{-4}, 1.66×10^{-2}, and 0.527 W for 60, 300, and 1000 rpm, respectively. The input energies were very small and might be easily balanced by thermal stat. So the degradation effect exerted by the mixer might mainly due to stir and stretch (Casale & Porter, 1978; Floury et al., 2002) rather than by increasing temperature. The input energies of this mixed system are dependent on the power coefficient which is proportional

to the exponent two of the rotation speed *r*. Therefore, increased rotation speed will enhance the power input to the system or increase the efficiency of stretch. However, the rotation speed should not be too high to generate a vortex, because with an increase in mixer speed, the resistance of the medium to the rotation of the mixer increases as it is induced by turbulization of the boundary layer and the formation of a turbulent wake in the zone behind the moving blades. Other means to increase the shearing effects are to provide conditions to work on the polymer such as the strong elongational flow encountered by the polymer at the entrance of the valve of the high pressure homogenizer device (Floury et al., 2002) or employing a homogenizer in the system instead of a mixer.

3.2. Effect of treatment time

Fig. 4(a) shows the effect of ultrasonic radiation time of 1, 2, and 4 min on the mean diameter change of chitosan–TPP nanoparticle at 48 W at 25 °C. The results showed that the mean diameter of nanoparticle decreased with increasing ultrasonic time. Fig. 4(b) shows the effect of mechanical shearing time of 1, 2, and 4 min on the change of chitosan–TPP nanoparticle at 1000 rpm at 25 °C. The results showed that the mean diameter of nanoparticle that was mechanically sheared for 1 or 2 min is smaller than that sheared for 4 min. Results in Fig. 4(c) shows that increased ultrasonic radiation time decreased the polydispersity of resulted nanoparticle from 0.438 to 0.436 and to 0.388. Results in Fig. 4(d) shows the effects of different shearing time on the polydispersity of the resulted nanoparticle. The polydispersities were 0.525, 0.530, and 0.528 for those subjected to 1, 2, and 4 min at 1000 rpm, respec-

tively. The polydispersities for those sheared for 1 min were the smallest whereas, for those sheared for 2 min were the largest.

The inconsistent results of the effect of reaction time on the mean particle size of resulting chitosan–TPP nanoparticle shown in Fig. 4(a) and (b) may be due to different degradation mechanisms of chitosan molecules and different size of degraded chitosan molecules participating in the ionotropic gelation chitosan–TPP nanoparticle formation mentioned in previous section. The longer the ultrasonic radiation treatment, the more the energy input thus producing more cavitation effect, therefore, ending up in smaller degraded molecules (Chen, Chang, & Shyur, 1997) and thus decreased mean nanoparticle size (Gan et al., 2005) shown in Fig. 4(a). The results shown in Fig. 4(a) were consistent with the report of Lan et al. (2004). However, results in Fig. 4(b) shows that mean particle size of that mechanically sheared for 1 or 2 min is smaller than that sheared for 4 min. This may be due to the fact that during the beginning 1 or 2 min of mechanical shearing, the effect of shearing was more pronounced than the effect of interpenetration entanglement. This resulted in the torn fragment that participated in the ionotropic gelation with TPP and formed smaller chitosan–TPP nanoparticle. However, further shearing the entanglement effect might overwhelm the torn effect. This might result in aggregated chitosan clusters. The aggregated chitosan cluster then underwent ionotropic gelation with TPP to form bigger nanoparticle, therefore, the mean particle size of that mechanically sheared for 1 or 2 min is smaller than that sheared for 4 min.

The decrease in polydispersity shown in Fig. 4(c) was similar to the decreases in polydispersity reported by Chen
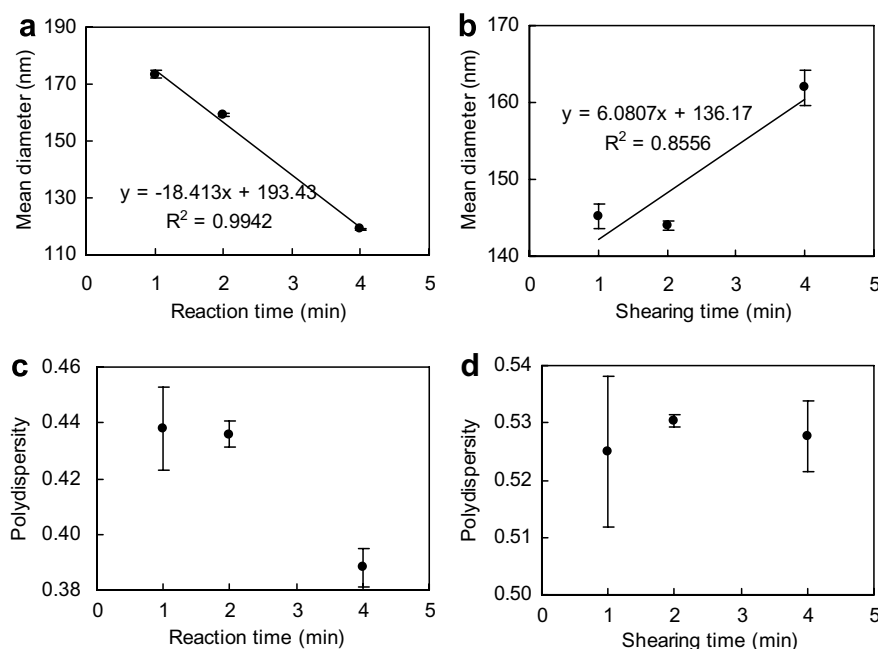

Fig. 4. Effects of reaction time of ultrasonic radiation (a), (c) and mechanical shearing time (b), (d) onto 2 mg/ml chitosan solution at 48 W and 1000 rpm, respectively, at 25 °C on the mean diameter (a), (b) and polydispersity (c), (d) of ionotropic gelation chitosan–sodium tripolyphosphate nanoparticles.

et al. (1997). This may be due to the longer radiation treatment time, the more the cavitation energy input into the solution, this will decrease the M_w and their distributions thus decreasing the polydispersity. The results indicated that the M_w of the cavitation bombardment fragments of chitosan determines the size and polydispersity of the resulted chitosan–TPP nanoparticle. The polydispersities were 0.525, 0.530, and 0.528 for those subjected to 1, 2, and 4 min at 1000 rpm, respectively. The polydispersities for those sheared for 1 min were the smallest whereas, for those sheared for 2 min was the largest. Although the average size of the torn fragment decreased with increasing shearing time (Fig. 4(b)), however, the polydispersity of the nanoparticle prepared from solution that has been sheared for 2 min were larger than that sheared for 1 min. This might be indicated that there are some larger nanoparticles in the supernatant, therefore, the polydispersity increased. The pattern of changing polydispersity shown in Fig. 4(d) was similar to those reported in Chen, Chang, and Shyur (1998). The reason that the polydispersity of the nanoparticle prepared from solution that has been sheared for 4 min were smaller than that sheared for 2 min might be due to the distribution of the aggregated chitosan cluster were smaller for these sheared for 4 min than that has been sheared for 2 min. The sheared for 2 min one might contain small and large particle in the supernatant after centrifuging treatment.

3.3. Effect of chitosan concentration

Fig. 5(a) shows the effect of chitosan concentration of 1, 2, 4, and 10 mg/ml on the changes of mean diameter of

chitosan–TPP nanoparticle treated with 29 W ultrasonic radiation for 4 min at 25 °C. The results in Fig. 5(a) shows that the mean diameter of resulted nanoparticle increased with increasing chitosan concentration. Fig. 5(b) shows the effect of chitosan concentration of 1, 2, 4, and 10 mg/ml on the change of mean diameter of chitosan–TPP nanoparticle treated with 1000 rpm shearing for 4 min at 25 °C. The results in Fig. 5(b) shows that the mean diameter of resulted nanoparticle increased also with increasing chitosan concentration. Results in Fig. 5(c) and (d) shows that increased the chitosan concentration, increased the polydispersity of resulted nanoparticle. The polydispersity increased from 0.240 to 0.371, 0.523, and 0.630 for 1, 2, 4, and 10 mg/ml chitosan solution, respectively, that were subjected to 29 W ultrasonic radiation for 4 min at 25 °C (Fig. 5(c)). The polydispersity increased from 0.400 to 0.523, 0.583, and 0.711 for 1, 2, 4, and 10 mg/ml chitosan solution, respectively, that was subjected to 1000 rpm shearing for 4 min at 25 °C (Fig. 5(d)).

Results in Fig. 5(a) and (b) were similar to those of Gan et al. (2005) and Grenha et al. (2005). This may be due to the fact that the higher the chitosan concentration, the less the average energy exerted on chitosan molecules (Chen et al., 1997). Lower cavitation energy and lower shearing and tearing energy will result in less number and bigger fragments of chitosan molecules (Chen et al., 1997, 1998; Tsaih et al., 2004) to undergo ionotropic gelation with TPP to form bigger nanoparticle. Results in Fig. 5(c) were similar to those of Chen et al. (1997). This may be due to the fact that radiation time needed to narrow down the polydispersity was shorter for lower concentration solutions than that for higher concentration ones. Therefore,
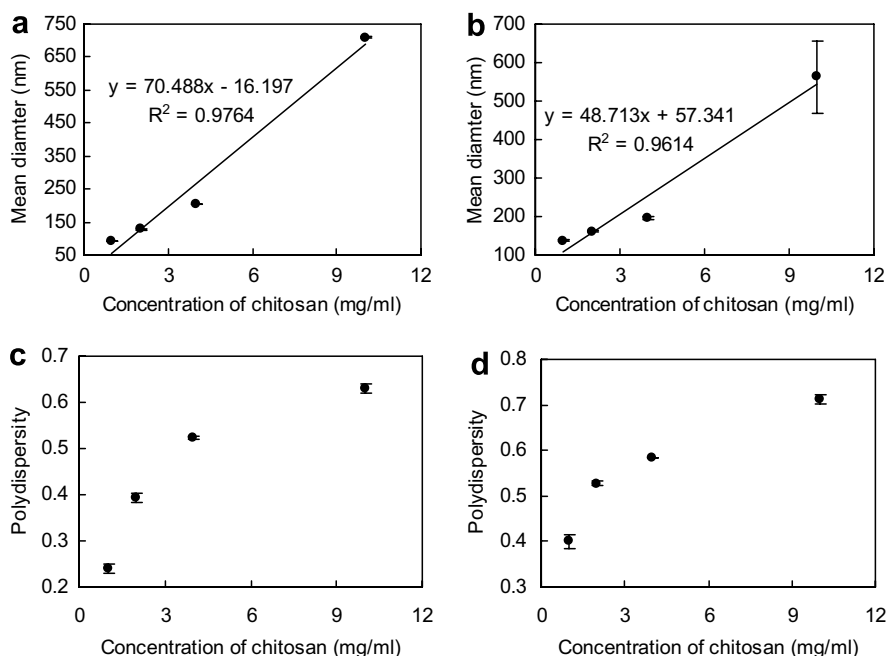

Fig. 5. Effects of concentration of chitosan solution ultrasonic radiation at 29 W (a), (c) and mechanical shearing at 1000 rpm (b), (d) onto 2 mg/ml chitosan solution at 25 °C for 4 min on the mean diameter (a), (b) and polydispersity (c), (d) of ionotropic gelation chitosan–sodium tripolyphosphate nanoparticles.

polydispersity increased with increasing concentration of chitosan solution. Results in Fig. 5(d) were similar to those of Chen et al. (1998). It could be attributed to the time needed to narrow down the polydispersity difference between low and high concentration solutions just mentioned.

3.4. Effect of solution temperature

Fig. 6(a) shows the effect of solution temperature of 4, 25, and 45 °C on the mean diameter change of chitosan–TPP nanoparticle treated with 29 W ultrasonic radiation onto 2 mg/ml chitosan solution for 4 min. The results showed that increasing temperature of chitosan solution decreased the mean diameter of resulted nanoparticle. Results in Fig. 6(b) shows the effect of solution temperature of 4, 25, and 45 °C on the mean diameter change of chitosan–TPP nanoparticle treated with 1000 rpm shearing onto 2 mg/ml chitosan solution for 4 min. The results indicated that the size of chitosan–TPP nanoparticle obtained at 25 °C solution was bigger than that obtained at 4 °C solution which in turn was larger than that obtained at 45 °C solution. The effects of solution temperature of 4, 25, and 45 °C on the polydispersity of chitosan–TPP nanoparticle exerted by cavitation or by stretching are shown in Fig. 6(c) and (d), respectively. Both results showed that increased the temperature of chitosan solution, decreased the polydispersity of resulted nanoparticle. The polydispersity decreased from 0.433 to 0.393 and to 0.371 for those ultrasonic radiation at 4, 25, and 45 °C, respectively (Fig. 6(c)), whereas the polydispersity decreased from 0.551 to 0.528 and to 0.523 for those stretched at 4, 25, and 45 °C, respectively (Fig. 6(d)).

The effects of solution temperature on the size of chitosan–TPP nanoparticle were different between nanoparticle obtained by cavitation effect and that obtained by stretching effect. The reasons are that the higher the solution temperature, the smaller the mean diameter of nanoparticle obtained by cavitation effect. This may be due to the fact that the higher the solution temperature, the lower the solution viscosity which facilitates the sporadic cavitation effect exerted on the chitosan molecules and degraded the chitosan molecules into smaller debris. The small chitosan debris resulted in small diameter of nanoparticle. Result in Fig. 6(a) is similar to that reported in Cao et al. (2005). They reported that the particle size of hydroxyapatite nanoparticle prepared by ultrasonic treatment decreased with increasing solution temperature. Results in Fig. 6(b) shows that the size of chitosan–TPP nanoparticles obtained at 25 °C solution was bigger than that obtained at 4 °C solution which in turn was larger than that obtained at 45 °C solution. This may be due to the fact that the higher the solution temperature, the lower the solution viscosity. Lower viscosity solution will facilitate the entanglement of some chitosan molecules with each other or with those torn fragments to form aggregated chitosan clusters. The aggregated chitosan cluster then ionotropically gelled with TPP to form bigger nanoparticles. Therefore, the higher the solution temperature, the larger the nanoparticle will form. The reason that nanoparticle obtained at 45 °C was the smallest among these three temperature solutions may be due to the fact that the larger nanoparticle species was removed during centrifugation treatment thus the remaining particles were smaller than that obtained from solution temperature of 4 °C or from 25 °C ones. Results in Fig. 6(c) were similar to those of Chen et al. (1997). This may be due to the fact
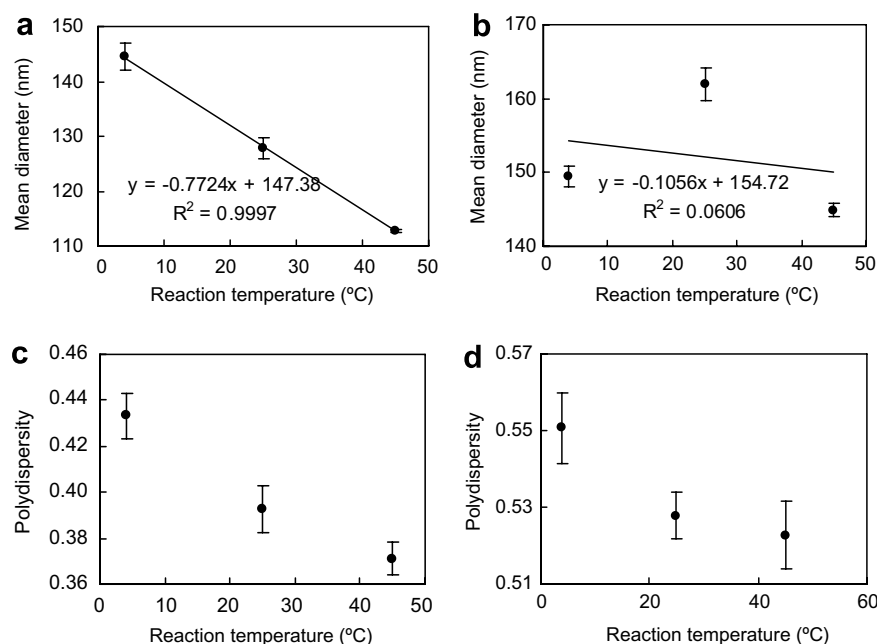

Fig. 6. Effects of the reaction temperature of ultrasonic radiation at 29 W (a), (c) and mechanical shearing at 1000 rpm (b), (d) for 4 min on the mean diameter (a), (b) and polydispersity (c), (d) of ionotropic gelation chitosan–sodium tripolyphosphate nanoparticles.

that the higher the solution temperature, the lower the solution viscosity which facilitates the sporadic cavitation effect exerted on the chitosan molecules thus resulting in decreasing diameter of nanoparticle and the polydispersity with increasing solution temperature. Results in Fig. 6(d) also shows that increased the temperature of chitosan solution, decreased the polydispersity of resulted nanoparticle. Chen et al. (1998) showed similar patterns. Effect of solution temperature on mean diameter shown in Fig. 6(b) was different from the effect of solution temperature on polydispersity as shown in Fig. 6(d). It could be attributed to that torn and/or stretch then centrifugation treatment, the bigger nanoparticle species (resulted of sheared at 25 °C) or the smaller species (the even bigger species resulted of shearing at 45 °C was removed) are the majority of the resulted species after treatment thus resulting in lower value of polydispersity. Results in Fig. 6(d) were similar to those of Chen et al. (1998).

4. Conclusion

The particle size of ionotropic gelation chitosan–TPP can be manipulated by using different mechanical energies such as ultrasonic radiation or mechanical shearing, different treatment times, different chitosan concentrations, and different solution temperatures.

Ultrasonic radiation or mechanical shearing treatment resulted in different nanoparticle size and different reduction rate of nanoparticle during treatment. This may be due to different degradation mechanisms of chitosan molecules and different size of degraded chitosan molecules participating in the ionotropic gelation with TPP molecules. The degradation of chitosan molecules by ultrasonic radiation is mainly caused by cavitation effect whereas, the degradation by mechanical shearing is mainly caused by tearing and and/or stretching effect.

Effect of solution temperature on resulted nanoparticle size by ultrasonic treatment or by mechanical shearing was different. The higher the solution temperature, the lower the solution viscosity which facilitates the sporadic cavitaion effect exerted on the chitosan molecules thus mean diameter of nanoparticle decreasing with increasing solution temperature. However, lower viscosity solution facilitates the entanglement of chitosan to form aggregated chitosan clusters. The aggregated chitosan cluster was then ionotropically gelled with TPP to form bigger nanoparticle. The reason that nanoparticle obtained at 45 °C was the smallest among them may be due to the largest nanoparticle being removed during centrifugation treatment.

The effects of concentration of chitosan or solution temperature on polydispersity of resulted nanoparticle by ultrasonic treatment or by mechanical shearing was similar whereas, the effects of input energy (in terms of W or shearing speed) or shearing time on polydispersity of resulted nanoparticle by ultrasonic treatment or by mechanical shearing was different. Higher input energy or longer treatment time will result in smaller polydispersity by ultrasonic treatment whereas, the effect of input energy in terms of shearing speed or treatment time on polydispersity by mechanical shearing did not show any trends. It depended on the different size of degraded chitosan molecules participating in the ionotropic gelation with TPP molecules and the larger nanoparticle may be removed during centrifugation treatment.

References

Agnihotri, S. A., Mallikarjuna, N. N., & Aminabhavi, T. M. (2004). Recent advances on chitosan-based micro- and nanoparticles in drug delivery. *Journal of Controlled Release, 100*, 5–28.

Azbel, D. S., & Cheremisinoff, N. P. (1983). *Fluid mechanics and unit operations*. Michigan: Ann Arbor Science Publishers, pp. 721–737.

Banerjee, T., Mitra, S., Singh, A. K., Sharma, R. K., & Maitra, A. (2002). Preparation, characterization and biodistribution of ultrafine chitosan nanoparticles. *International Journal of Pharmaceutics, 243*, 93–105.

Baxter, A., Dillon, M., Taylor, K. D. A., & Roberts, G. A. F. (1992). Improved method for i.r. determination of the degree of *N*-acetylation of chitosan. *International Journal of Biological Macromolecules, 14*, 166–169.

Calvo, P., Remunan-Lopez, C., Vila-Jato, J. L., & Alonso, M. J. (1997). Novel hydrophilic chitosan–polyethylene oxide nanoparticles as protein carriers. *Journal of Applied Polymer Science, 63*, 125–132.

Cao, L. Y., Zhang, C. B., & Huang, J. F. (2005). Influence of temperature, [Ca^{2+}], Ca/P ratio and ultrasonic power on the crystallinity and morphology of hydroxyapatite nanoparticles prepared with a novel ultrasonic precipitation method. *Materials Letters, 59*, 1902–1906.

Casale, A., & Porter, P. (1978). *Polymer stress reactions* (Vol. 1). New York: Academic Press.

Chen, R. H., Chang, J. R., & Shyur, J. S. (1997). Effects of ultrasonic conditions and storage in acidic solutions on changes in molecular weight and polydispersity of treated chitosan. *Carbohydrate Research, 299*, 287–294.

Chen, R. H., Chang, J. R., & Shyur, J. S. (1998). Effect of shear conditions and storage in acidic solutions on molecular weight and polydispersity of treated chitosans. *Journal of Fisheries Society of Taiwan, 25*(3), 219–229.

Desai, M. P., Labhasetwar, V., Walter, E., Levy, R. J., & Amidom, G. L. (1997). The mechanism of uptake of biodegradable microparticles in caco-2 cells is size dependent. *Pharmaceutical Research, 14*, 1568–1573.

Floury, J., Desrumaus, A., Axelos, M. A. V., & Legrand, J. (2002). Degradation of methylcellulose during ultra-high pressure homogenization. *Food Hydrocolloids, 16*, 47–53.

Gan, Q., Wang, T., Cochrane, C., & McCrron, P. (2005). Modulation of surface charge, particle size and morphological properties of chitosan–TPP nanoparticles intended for gene delivery. *Colloids and Surfaces B: Biointerfaces, 44*, 65–73.

Grenha, A., Seijo, B., & Remuñán-López, C. (2005). Microencapsulated chitosan nanoparticles for lung protein delivery. *European Journal of Pharmaceutical Sciences, 25*, 427–437.

Grönroons, A., Pirkonen, P., Heikkinen, J., Ihalainen, J., Mursunen, H., & Sekki, H. (2001). Ultrasonic depolymerization of aqueous polyvinyl alcohol. *Ultrasonics Sonochemistry, 8*, 259–264.

Kurita, K., Tomita, K., Ishii, S., Nishimura, S. I., & Shimoda, K. (1993). β-Chitin as a convenient starting material for acetolysis for efficient preparation of *N*-acetylchitooligosaccharides. *Journal of Polymer Science Part A-Polymer Chemistry, 31*, 2393–2395.

Lan, J., Yang, Y., & Li, X. (2004). Microstructure and microhardness of SiC nanoparticles reinforced magnesium composites fabricated by ultrasonic method. *Materials Science and Engineering A, 386*, 284–290.

Lee, D.-W., Powers, K., & Baney, R. (2004). Physicochemical properties and blood compatibility of acylated chitosan nanoparticles. *Carbohydrate Polymers, 58*, 371–377.

Lee, S. T., Mi, F. L., Shen, Y. J., & Shyu, S. S. (2001). Equilibrium and kinetic studies of copper (II) ion uptake by chitosan–tripolyphosphate chelating resin. *Polymer, 42*, 1879–1892.

López-León, T., Carvalho, E. L. S., Seijo, B., Ortega-Vinuesa, J. L., & Bastos-González, D. (2005). Physicochemical characterization of chitosan nanoparticles: Electrokinetic and stability behavior. *Journal of Colloid and Interface Science, 283*, 344–351.

Sarmento, B., Ferreira, D., Veiga, F., & Ribeiro, A. (2006). Characterization of insulin-loaded alginate nanoparticles produced by ionotropic pre-gelation through DSC and FTIR studies. *Carbohydrate Polymers, 66*, 1–7.

Shu, X. Z., & Zhu, K. J. (2000). A novel approach to prepare tripolyphosphate/chitosan complex beads for controlled release drug delivery. *International Journal of Pharmaceutics, 201*, 51–58.

Tang, E. S. K., Huang, M., & Lim, L. Y. (2003). Ultrasonication of chitosan and chitosan nanoparticles. *International Journal of Pharmaceutics, 265*, 103–114.

Tsaih, M. L., & Chen, R. H. (1999). Molecular weight determination of 83% degree of deacetylation chitosan with non-gaussian and wide range distribution by high-performance size exclusion chromatography and capillary viscometry. *Journal of Applied Polymer Science, 71*, 1905–1913.

Tsaih, M. L., & Chen, R. H. (2003). The effect of reaction time and temperature during heterogenous alkali deacetylation on degree of deacetylation and molecular weight of resulted chitosan. *Journal of Applied Polymer Science, 88*, 2917–2923.

Tsaih, M. L., Tseng, L. Z., & Chen, R. H. (2004). Effects of removing small fragment with ultrafiltration treatment and ultrasonic conditions on degradation kinetics of chitosan. *Polymer Degradation and Stability, 86*, 25–32.

van der Lubben, I. M., Verhoef, J. C., Borchard, G., & Junginger, H. E. (2001). Chitosan for mucosal vaccination. *Advanced Drug Delivery Reviews, 52*, 139–144.

Vila, A., Sánchez, A., Janes, K., Behrens, I., Kissel, T., Vila Jato, J. L., et al. (2004). Low molecular weight chitosan nanoparticles as new carriers for nasal vaccine delivery in mice. *European Journal of Pharmaceutics and Biopharmaceutics, 57*, 123–131.

Yuan, X. B., Li, H., & Yuan, Y. B. (2006). Preparation of cholesterol-modified chitosan self-aggregated nanoparticles for delivery of drugs to ocular surface. *Carbohydrate Polymers, 65*, 337–345.